Atom Lithography with a Holographic Light Mask

M. Mützel, S. Tandler, D. Haubrich, and D. Meschede

Institut für Angewandte Physik, Universität Bonn, Wegelerstrasse 8, D-53115 Bonn, Germany

K. Peithmann,* M. Flaspöhler, and K. Buse*

Universität Osnabrück, Fachbereich Physik, Barbarastrasse 7, D-49069 Osnabrück, Germany

In atom lithography *with optical masks,* deposition of an atomic beam on a given substrate is controlled by a standing light-wave field. The lateral intensity distribution of the light field is transferred to the substrate with nanometer scale. We have tailored a complex pattern of this intensity distribution through diffraction of a laser beam from a hologram that is stored in a photorefractive crystal. This method can be extended to superpose 1000 or more laser beams. The method is furthermore applicable during growth processes and thus allows full 3D structuring of suitable materials with periodic and nonperiodic patterns at nanometer scales.

Introduction.—Generation of complex nanoscale structures is usually performed in a multistep procedure. For a given structure it involves the transfer of a mask into a resist either through direct contact or by optical imaging. The chemically modified surface is then subjected to a series of physical and chemical processes in order to prepare a desired structure. These methods are overwhelmingly successful and perfectly adapted to the generation of planar structures such as required in microelectronic circuitry. However, they also exhibit certain shortcomings which limit their usefulness for other problems. For instance, their impact is confined to surfaces, and thus full 3D structuring can be achieved only by even more processing steps which makes the procedure cumbersome. Here we present a method that may overcome this problem by inducing a tailored complex pattern into the density distribution of atomic beams at nanometer scale. This modulation is caused by light forces of a coherent multibeam light field that is reconstructed from a hologram that is stored in a photorefractive crystal. This light modulation can be transferred to the lateral composition of compound crystals during growth. In the third dimension the composition can be varied conventionally through regulation of the contributing constituents, and hence this method may in principle be extended to grow, e.g., photonic crystals with nanoscale structure in all three dimensions.

The nanofabrication method using a neutral atomic beam is named "neutral atom lithography" [1,2]. It was introduced as an application of atom optics where patterned atomic beams are used to create permanent structures on surfaces. Patterning can be achieved by manipulating internal or external atomic degrees of freedom. In our case, i.e., atom lithography with optical masks, optical dipole forces are utilized to concentrate atoms near the nodes of a blue detuned standing light-wave field. Light forces of a plane standing wave have been applied in several laboratories to create arrays of straight parallel lines at subnanometer scales and to investigate basic properties of

atom nanofabrication processes [3–5]. Two variants can be distinguished: One method (resist technique) uses a beam of reactive atoms (metastable rare gases [6], alkali beams [7]) to chemically modify a suitable resist such as a monolayer of organic molecules. This chemical pattern is subsequently prepared by conventional etching methods in close analogy to optical or *e*-beam lithography. In another approach (direct deposition) the structure is directly grown from the atoms deposited in a preselected pattern [4]. For this case a minimal structural width of 20 nm has been reported for chromium atoms [8].

It was furthermore shown that laser beams could be superposed through an arrangement of mirrors such that two-dimensional patterning with three- or fourfold symmetry was achieved [9,10]. Generation of even higher degrees of complexity with this method, however, is limited by the accompanying growth in complexity of the experimental arrangement. In this report we show that already a single hologram that is stored in a photorefractive crystal offers an equivalent of superposing numerous individual light beams to form a lens-free complex light mask that can successfully be used in atom nanofabrication. We furthermore show that weak modulation of the light field is sufficient for atom nanofabrication which significantly simplifies the design of the light field intensity distribution.

Experimental.—For atomic imaging we use a thermal cesium atomic beam which is transversely collimated by laser cooling methods (Fig. 1, side view) to a remaining divergence below 1 mrad. The diameter of the atomic beam is defined by an aperture of 1 mm and travels 1 mm off the crystal. When it is exposed to the light mask, optical dipole forces modify atomic trajectories and cause a transversal density modulation of the atomic beam. The structure of this modulation replicates the general pattern of the intensity distribution of the light field.

The atomic beam with modulated intensity distribution is deposited on a Si substrate covered with a self-assembled
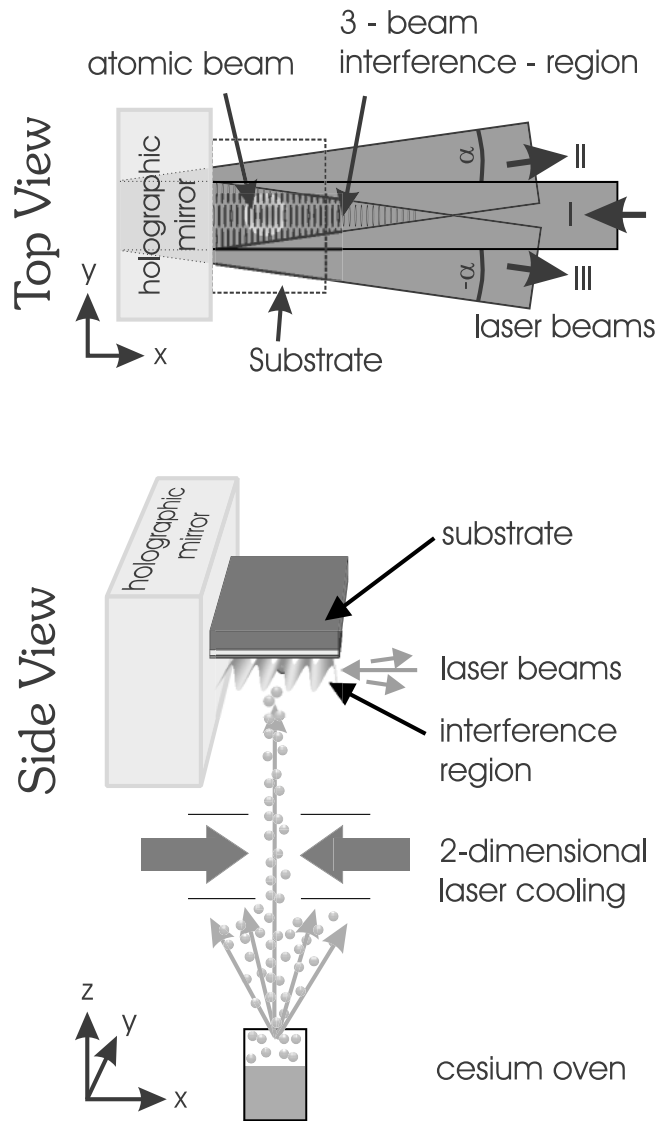
FIG. 1. Experimental setup for atom nanofabrication with a holographic mirror. The thermal cesium atomic beam is collimated by two-dimensional laser cooling before it passes the light mask (side view). The light mask is generated by interference of the readout beam I and beams II and III that are reconstructed by the holographic mirror (top view).

monolayer (SAM) of nonanthiole on a 30 nm gold layer [7]. It is exposed for typically 90 s at a flux density of 5×10^{12} s^{-1} cm^{-2} corresponding to about 1 ML of cesium on the substrate surface. The structure is then transferred to the gold layer through wet etching processes. Such a method was already used for the production of periodic nanostructures with a plane standing wave generated with a laser beam reflected by a flat mirror [5]. In our case a volume phase hologram diffracts the incoming laser beam into multiple laser beams where for the sake of simplicity we have restricted our experiment to two beams only. They interfere with the incoming laser beam forming a light field with two-dimensional intensity modulation (Fig. 1, top view). All information about the light mask

intensity distribution is stored in the hologram which we have recorded in iron-doped photorefractive LiNbO$_3$.

The hologram constructed here is called "volume hologram" because efficient reconstruction of any signal wave field requires Bragg matching of the incoming beam, making the hologram highly selective to the wavelength or direction of the reference light beam. Such a hologram can be recorded beam by beam with a density of, e.g., 1 beam per mrad for a 1 mm thick crystal which makes efficient construction of tailored light masks possible.

For hologram recording the crystal is heated to 180 °C. A Ti:sapphire laser beam with a power of typically 2.0 W is spatially filtered, expanded to a diameter of about 4 mm, and split into three separate beams (I, II, and III) with intensities around 6 W/cm^2 each. All beams are polarized perpendicularly to the plane of incidence. During recording all three beams interfere within the sample for about 3 h, since the sensitivity of LiNbO$_3$:Fe for near-infrared light is rather low [11]. To ensure a stable position of the interference pattern over this long time an active mechanical stabilization of the entire setup is employed [12]. After cooling to room temperature the hologram is finally developed with light from a tungsten lamp. Due to recording at high temperature, the refractive index pattern is fixed with an estimated lifetime of 20 years.

Because of thermal expansion of the crystal, recording wavelength and readout wavelength do not coincide. Thus, during the recording process, the Ti:sapphire laser is set to a wavelength 0.58 nm longer than that of the cesium D$_2$ resonance at 852.1 nm. This leads to an optimum diffraction efficiency of the volume hologram during the readout process at lower temperatures. Before insertion of the crystal into the vacuum chamber used for the atom nanofabrication we checked the dependence of the diffraction efficiency on temperature and on the angle of incidence. From these results we found that the hologram works at best for perpendicular incidence of the reading beam at a temperature of 35 °C with diffraction efficiencies of at least 13% for beams II and III.

The power of the readout laser beam is 18 mW with a positive detuning δ of 600 MHz from the cesium D$_2$ line (852.1 nm). The readout beam is a Gaussian laser beam with a diameter $2w_z$ of 170 μm in the direction of the atomic beam (z axis), and $2w_\perp$ of about 1.6 mm transverse to the atomic beam. This makes certain that the atomic beam (diameter 1 mm) is fully covered by all contributing laser beams. The angle α between the incoming beam and each of the two diffracted beams is 35 mrad, the power of the diffracted beams measured in units of the incoming laser beam power is 18% and 20%, respectively. Multiple beam interference leads to a contrast exceeding 99% in the light intensity distribution of the mask. An additional weak laser beam (3%) is observed that modifies the light mask. This beam is attributed to an additional reflection hologram that is written by back reflection of recording beam I at the rear crystal surface.

Since the detuning δ is much larger than the natural linewidth of the cesium resonance ($\gamma = 5.22$ MHz), the optical dipole force on the atoms can be written as [13]

$$F = -\frac{h\gamma^2}{8\delta I_{sat}} \nabla I(\mathbf{r}),$$

where I_{sat} is the saturation intensity of the atomic transition, and $I(\mathbf{r})$ is the intensity distribution of the light mask. In the vicinity of the minima of the light mask, the local intensity distribution can be approximated as a harmonic potential. Thus the atoms are focused towards the minima of the standing light wave [14]. The theoretical focal lengths of those local light-wave lenses vary from a few microns to some 100 μm for atoms with a typical velocity of 300 m/s, depending on the local contrast of the light mask. However, we found in numerical simulations as well as empirically that a distance of $0-80$ μm between the substrate and the center of the light mask is suited for the generation of high contrast patterns.

The intensity distribution $I(\mathbf{r})$ of the light mask is derived from interference of all contributing laser beams. Since all laser beams propagate perpendicular to the atomic beam, the interference term F depends only on the coordinates x and y, while in the z direction the light intensity follows a Gaussian profile:

$$I(\mathbf{r}) = I_0 \exp\left(-\frac{2z^2}{w_z^2}\right) \times F(x, y).$$

For simplicity we treat the interfering laser beams as plane waves $\varepsilon \exp(i\mathbf{k}\mathbf{r})$ in the x, y plane with position vector $\mathbf{r} = (x, y)$, wave vector $\mathbf{k} = (k_x, k_y)$, and complex amplitude ε. If the amplitudes ε_i of the diffracted beams $\varepsilon_i \exp(i\mathbf{k}_i\mathbf{r})$ are small compared to that of the readout beam $E_0 \exp(i\mathbf{k}_0\mathbf{r})$, mutual interference is proportional to $\varepsilon_j\varepsilon_i^*$ that yields a fixed but negligible speckle pattern. Thus the interference term F, which corresponds exactly to the intensity pattern in our experiment, can be approximated:

$$F(\mathbf{r}) = 1 + 2\,\mathrm{Re}\left\{\sum_i \frac{\varepsilon_i^*}{E_o} \exp[i(\mathbf{k}_o - \mathbf{k}_i)\mathbf{r}]\right\}$$

$$+ O\left(\frac{\varepsilon_i\varepsilon_j^*}{E_0^2}\right).$$

Each diffracted beam contributes linearly to the intensity pattern, which can be analyzed in terms of a Fourier composition where certain additional conditions apply since for a monochromatic light field all wave vectors $\mathbf{k}_i$ have identical lengths, and hence the selection of vectors $\mathbf{G}_i = (\mathbf{k}_o - \mathbf{k}_i)$ is restricted.

Results.—A typical result of our nanofabrication experiment with a holographically defined light mask is shown in Fig. 2. A 30 μm $\times$ 35 μm display window of the generated gold structure on a silicon wafer is visualized with the help of a high-aperture optical microscope. A two-dimensional pattern is observed: Horizontal lines with a periodicity of approximately $\lambda/2 = 426$ nm result from
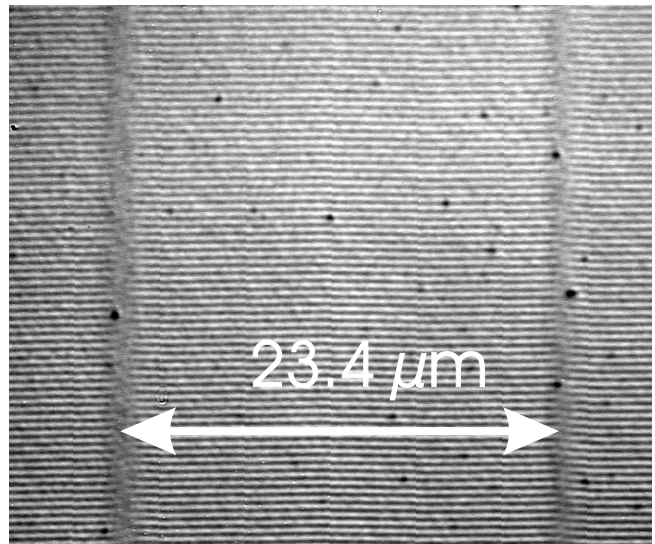

FIG. 2. Optical microscope picture of gold structures (bright regions) after processing.

interference of the incoming laser beam I with the two reflected laser beams II and III. The superposed pattern shows two vertical bands with 23.4 μm spacing which arise from an interruption of the vertical lines. These interruptions result from interference of the laser beams II and III. While the interference of only three beams would result in a pattern with constant 24.4 μm spacing between neighboring displacements, our samples show a modulation of this distance as a result of the additional fourth laser beam mentioned above. The observable dark dots in Fig. 2 are dust particles which accumulate to the substrate due to absence of protective measures.

Figure 3(a) shows a closeup of the displacement region presenting more details of the interruption zone. The $(3.6\ \mu\text{m})^2$ display window is recorded with an atomic force microscope (AFM). The AFM picture shows an interruption of the 30 nm high lines associated with a displacement in the vertical direction of half a period, or $\lambda/4$. We have also carried out numerical trajectory simulations
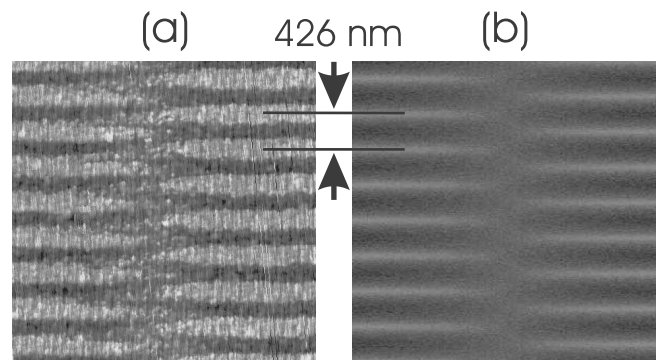

FIG. 3. (a) Atomic force microscope picture of generated gold structures (bright regions). (b) Numerical simulation of atomic flux density in the substrate plane. Bright regions indicate high atomic flux density.

by classically computing the dipole force acting onto the atoms passing through the light mask. We have used our experimental parameters to simulate 10^7 atomic trajectories, that represent the velocity distribution of our atomic beam. The result for the two-dimensional distribution of atomic flux density behind the light mask at the position of the substrate is shown in Fig. 3(b). Bright regions indicate high atomic flux density, where the gold is removed by wet etching. This simulation is in very good agreement with our experimental results.

Conclusion.—We have shown that a volume hologram provides sufficient modulation for a light mask to be used in atom nanofabrication and to fabricate a tailored structure. This experimental proof of the concept makes further developments feasible. (1) Holograms that yield on reconstruction several beams allow generation of complex light masks with periodic as well as with nonperiodic patterns, for instance for fabrication of quasicrystals. Furthermore, these 2D light masks can be used as complex light controlled phase holograms for coherent matter waves, capable of reconstructing atomic patterns with nanometer scale after passing through the light field. The validity of this approach was shown with a mechanical hologram by Fujita *et al.* [15]. (2) Reconstruction of waves from volume holograms requires fulfillment of the Bragg condition which allows multiplexing of several holograms, i.e., light masks that can be addressed by changing the readout angle or wavelength. Thus, e.g., three-dimensional structures can be made because it is easy to switch during the growth of the lithographic structure from one light mask to another. (3) Since beams of different wavelength can reconstruct different light masks at the same time, an atomic beam consisting of different atom species can be shaped atom selective.

An attractive application of hologram-assisted atomic beam lithography could be the fabrication of photonic crystals with diamond structure, for instance with $In_x Al_{1-x}As$, where In is accessible with light forces. This is, as far as we know, a unique feature of the novel approach presented here. These examples and the conducted experiments show the rich potential of combining atom nanofabrication with holographic light masks.

*Present address: Physikalisches Institut, Universität Bonn, Wegelerstrasse 8, D-53115 Bonn, Germany

[1] J. H. Thywissen *et al.,* J. Vac. Sci. Technol. B **15**, 2093 (1997).
[2] A. S. Bell *et al.,* Surf. Sci. **433–435**, 40 (1999).
[3] G. Timp *et al.,* Phys. Rev. Lett. **69**, 1636 (1992).
[4] J. J. McClelland, R. E. Scholten, E. C. Palm, and R. J. Celotta, Science **262**, 877 (1993).
[5] F. Lison *et al.,* Appl. Phys. B **65**, 419 (1997).
[6] K. K. Berggren *et al.,* Science **269**, 1255 (1995).
[7] M. Kreis *et al.,* Appl. Phys. B **63**, 649 (1996).
[8] W. R. Anderson, C. C. Bradley, J. J. McClelland, and R. J. Celotta, Phys. Rev. A **59**, 2476 (1999).
[9] R. Gupta, J. J. McClelland, Z. J. Jabbour, and R. J. Celotta, Appl. Phys. Lett. **67**, 1378 (1995).
[10] U. Drodofsky *et al.,* Appl. Phys. B **65**, 755 (1997).
[11] K. Peithmann, A. Wiebrock, and K. Buse, Appl. Phys. B **68**, 777 (1999).
[12] S. Breer *et al.,* Rev. Sci. Instrum. **69**, 1591 (1998).
[13] J. Dalibard and C. Cohen-Tannoudji, J. Opt. Soc. Am. B **2**, 1707 (1985).
[14] J. J. McClelland, J. Opt. Soc. Am. B **12**, 1761 (1995).
[15] J. Fujita *et al.,* Nature (London) **380**, 691 (1996).